



Trade-linked shipping CO₂ emissions

Xiao-Tong Wang^{1,2}, Huan Liu^{1,2}✉, Zhao-Feng Lv¹, Fan-Yuan Deng¹, Hai-Lian Xu¹, Li-Juan Qi¹, Meng-Shuang Shi¹, Jun-Chao Zhao¹, Song-Xin Zheng¹, Han-Yang Man¹ and Ke-Bin He¹

The ambitious targets for shipping emissions reduction and challenges for mechanism design call for new approaches to encourage decarbonization. Here we build a compound model chain to deconstruct global international shipping emissions to fine-scale trade flows and propose trade-linked indicators to measure shipping emissions efficiency. International maritime trade in 2018 contributes 746.2 Tg to shipping emissions of CO₂, of which 17.2% is contributed from ten out of thousands of trade flows at the country level. We argue that potential unfairness exists if allocating shipping emissions responsibility to bilateral traders due to external beneficiaries. However, a huge shipping emissions-reduction potential could be expected by optimizing international trade patterns, with a maximum reaching 38% of the current total. Our comprehensive modelling system can serve as a benchmark tool to support the construction of a systematic solution and joint effort from the shipping industry and global trade network to address climate change.

As a backbone of international trade and the global economy, maritime transport accounts for more than 80% of the world's trade by volume¹. Maritime trade emits billions of tons of shipping greenhouse gas (GHG) per year^{2–4}, equivalent to the sixth largest emitting country⁵, which is considered a major hindrance to keep warming under two degrees Celsius^{6–8}. To this end, the International Maritime Organization (IMO) announced an “Initial Strategy” on reduction of shipping GHG emissions, which set a target of at least a 50% reduction by 2050 (compared with 2008) and provided a wide list of candidate measures⁹. However, despite the existing energy efficiency improvement plans for the global fleet^{10–12}, there is still a lack of effective emissions-reduction mechanisms and of a clear implementation path. The past few years have witnessed continuously high global shipping CO₂ emissions². Moreover, an increase of ~10–30% of global shipping CO₂ emissions would be expected in 2050 compared with 2008 under a business-as-usual scenario².

Numerous studies have suggested that it is inadequate to achieve absolute emissions reductions solely by depending on global-collective ship technology iteration and operational measures^{13–16}. An effective and stable international cooperation regime is of equal importance. Currently there is still a lack of effective emissions-reduction measures and of a clear implementation path to achieve the ambitious goals.

Such a predicament calls for new perspectives to advocate for emissions reduction by elucidating the commercial drivers behind the fleet behaviour and shipping emissions as well as enhancing the transparency in what drives emissions. The regime of shipping emissions reduction has been discussed for decades. Beginning with the proposal of the eight options for shipping emissions responsibility allocation by the United Nations Framework Convention on Climate Change (UNFCCC)¹⁷, numerous efforts have been made to explore the rationality and justification of different options^{18–23}. Different allocation options may leave countries with vastly different emissions burdens, and currently there is no single option that is effective in terms of environment, law and fair burden sharing²⁰. This demonstrates the infeasibility of compulsory responsibility allocation and the necessity of new mechanism construction. Given that international trade is the driving force of shipping emissions, it

is essential to establish a fine-scale linkage between shipping emissions and maritime trade, as well as the drivers behind shipping emissions, to form a long-term and effective decarbonization path.

Recently, a few macroeconomic studies have investigated the shipping emissions characteristics linked with international trade^{19,24–28}, indicative of a growing focus on the trade-driven analysis of shipping emissions. However, these evaluations were conducted based on empirical parameters of shipping energy efficiency, which have poor linkage with actual ship activities. With the advent of the big data era, shipping emissions inventories developed based on observed ship activities from the ship automatic identification system (AIS) have improved accuracy and resolution^{2,29–33}, but these evaluations mostly have poor linkage with international trade. Only a few studies attempt to link shipping emissions with trade with ‘bottom-up’ evaluations, such as the cases of Brazil with its trading partners³⁴ and US–China bilateral trade³⁵. However, these methods used for limited bilateral pairs cannot be extended directly to the global scale, as they require abundant voyage-based ship cargo information that may be commercially sensitive or inaccessible. Thus, there is still a technical challenge in forming a comprehensive assessment of trade-linked shipping emissions involving all global bilateral traders.

Here we construct a compound technical framework with two ‘bottom-up’ models, namely the Voyage-based Shipping Emission Inventory Model (VoySEIM) and the Global Trade Emission Matrix of Shipping (GTEMS) model, to systematically investigate international maritime trade-linked shipping emissions with a target year of 2018. The model framework and data sources are described in the Methods. The VoySEIM is first developed to assess the international voyage-based shipping emissions and vessel energy efficiency operational indicator (EEOI; gCO₂ ton^{−1} per nautical mile (NM)) based on observed fleet activities from the AIS big data. Combined with the voyage-based EEOI, the GTEMS model is then constructed to estimate the international trade-linked shipping emissions driven by global bilateral trade flows. Shipping emissions contributions and trade-related emissions efficiencies are interpreted by shipping route, trade country and commodity. Finally, we investigate the shipping emissions-reduction potential from the perspective of global

¹State Key Joint Laboratory of ESPC, School of Environment, Tsinghua University, Beijing, China. ²These authors contributed equally: Xiao-Tong Wang, Huan Liu. ✉e-mail: liu_env@tsinghua.edu.cn

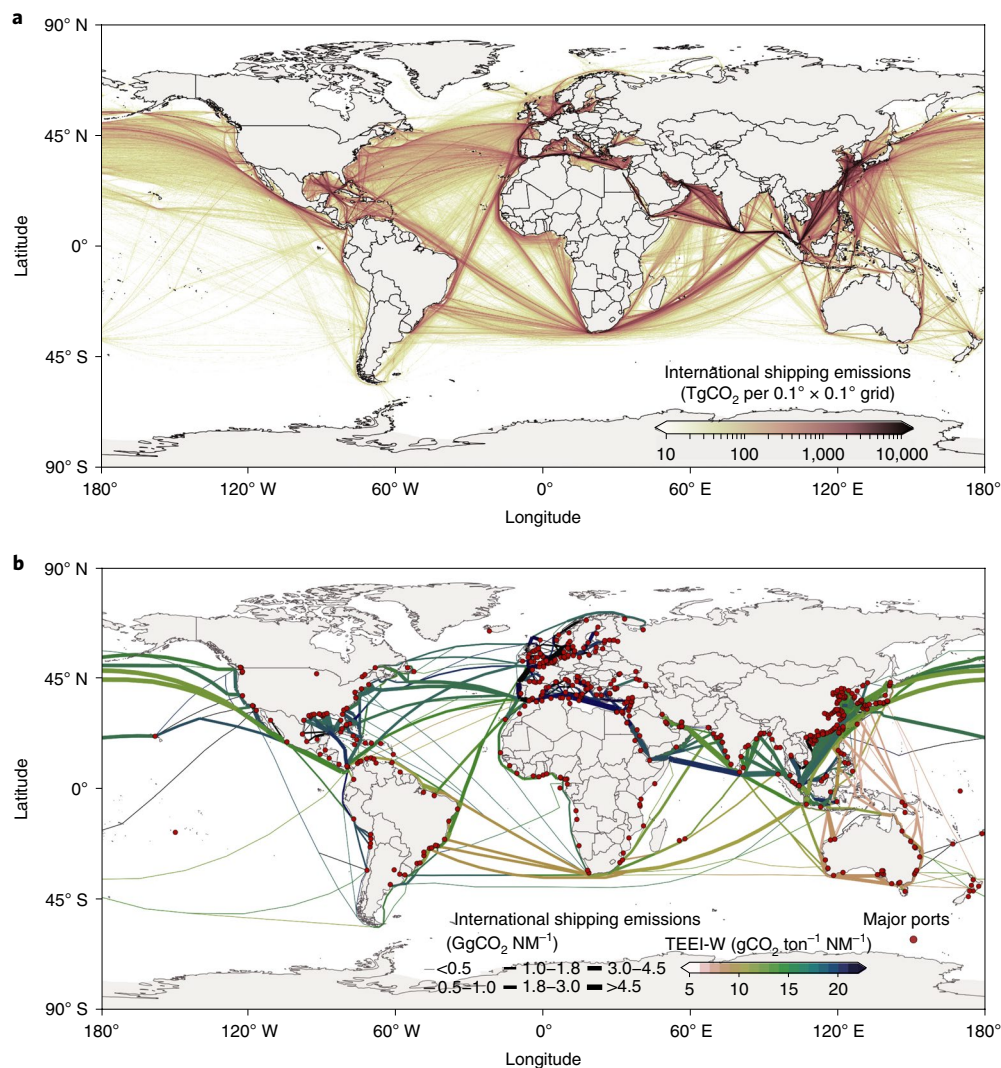


Fig. 1 | Distribution of international shipping emissions resulting from the VoySEIM and the GTEMS model. a,b, International shipping CO₂ emissions resulting from the VoySEIM (**a**) assessed by observed vessel voyages and from the GTEMS model (**b**) estimated based on bilateral trade flows. For **b**, the shipping route network is established based on the shortest paths of the world's major ports (the 'Shipping route distance' section in the Methods). The emissions intensity ($\text{gCO}_2 \text{NM}^{-1}$) represents the cumulative emissions of all trade transport vessels passing through each route segment, while the TEEI-W ($\text{gCO}_2 \text{ton}^{-1} \text{NM}^{-1}$) is the shipping emissions intensity versus the weight of all commodities transported. Maps are made with Natural Earth.

trade structure optimization as an application of the GTEMS model. The GTEMS model enables the integration of economics and environmental science methodologies, providing a new perspective for shipping emissions interpretation as well as for driving emissions-reduction potential. Descriptions of the uncertainties and model validation are included in the Methods.

Global map of international trade-linked shipping emissions

Figure 1 shows the spatial distribution of international shipping emissions on global maps resulting from the VoySEIM and the GTEMS model. The VoySEIM assesses gridded emissions for ~790,000 individual origin-destination (OD) voyages from a specific departure country to a specific arrival country based on minute-frequency AIS signals (Supplementary Fig. 1), accumulating to a global emissions inventory with high spatial resolution (Fig. 1a). Each OD voyage-based emissions are further used to estimate voyage-based EEOI, which is affected by vessel type, dead weight tonnage (DWT), capacity utilization, navigation distance and so on^{36,37} (Supplementary Discussion 1 and Supplementary Fig. 2). Benefiting from the heterogeneity of voyage-based EEOI, the

GTEMS model achieves the evaluation of international shipping emissions driven by ~1.2 million fine-scale global bilateral trade flows on a standardized global route network. Based on GTEMS, we estimate that international maritime trade in 2018 cumulatively contributed 746.2 Tg of shipping CO₂ emissions, which is comparable with the observed vessel voyages indicated by VoySEIM (727.3 Tg) as well as those informed by the fourth IMO GHG report² (detailed comparisons in Supplementary Table 1). Both models show dense shipping emissions on the circum-equatorial corridor, especially in East Asia, Southeast Asia, the Middle East and European waters. The highest emissions intensity of CO₂ reaches 22.1 $\text{GgCO}_2 \text{NM}^{-1}$ (Fig. 1b) for a route located near the Strait of Malacca, which as a major channel linking East Asia and Europe has been shown to suffer great atmospheric impacts and depositions from large amounts of shipping emissions³⁸.

To further interpret the trade-linked shipping emissions characteristics, the trade-emissions efficiency index by weight (TEEI-W; $\text{gCO}_2 \text{ton}^{-1} \text{NM}^{-1}$) is introduced to show the shipping emissions per unit distance of all commodities transported. Different from the vessel EEOI describing each individual voyage for each ship,

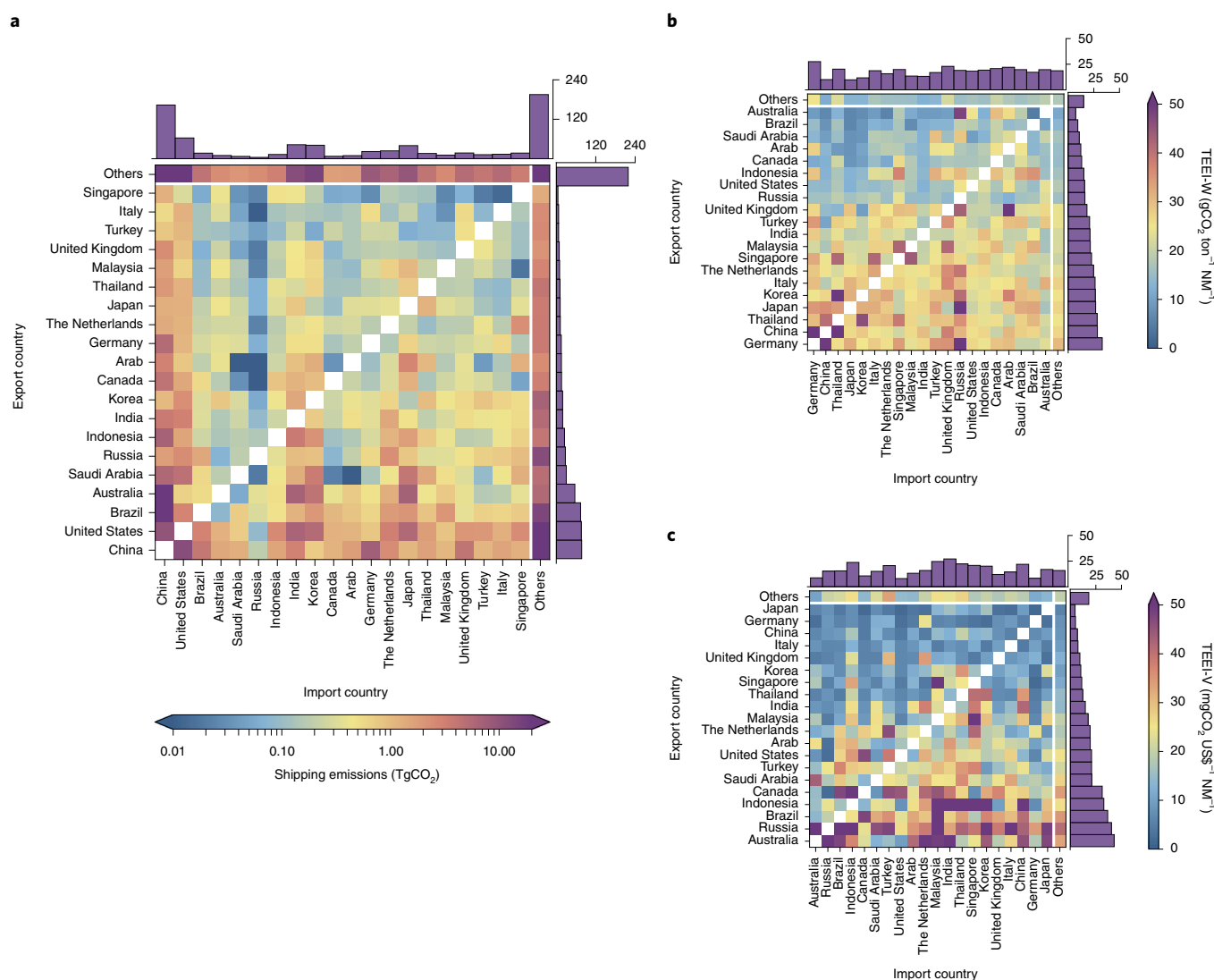


Fig. 2 | International shipping CO₂ emissions and trade-emissions efficiency matrix. **a**, Matrix of shipping emissions. **b**, Matrix of TEEL-W. **c**, Matrix of TEEL-V. The matrices reveal the estimated result for single-direction trade pairs, while the bars on the upper and right sides of each matrix refer to the accumulated emissions attributed to each country in **a** and average values of TEEL of each country in **b** and **c**. The heat map and bar plots share the same unit. Countries are arranged in descending order of trade export and those without notable shipping emissions are merged into 'others'. The top 30 bilateral emissions flows in **a** together with their trade value and weight are listed in Supplementary Table 2.

the TEEL-W illustrates emissions efficiencies from a trade perspective, taking into consideration the bilateral trade volume and structure, as well as the determined fleet size and voyage composition. Millions of shipping voyages operate with different EEOIs, departing from thousands of coastal ports and gathering on the main routes, ultimately resulting in heterogeneity in shipping emissions intensity and trade-emissions efficiency on different routes (Fig. 1b). The TEEL-W appears to be highest in Europe, where energy-intensive vessels such as containers and roll-on/roll-off (Ro-Ro) ships account for larger proportions of the transportation structure. In contrast, a lower TEEL-W is observed on routes in the Southern Hemisphere due to the frequent traffic of energy-efficient vessels such as bulk carriers. Although the total average TEEL-W for global fleets has generally shown a decreasing trend for the past few years and is expected to continuously decrease, the heterogeneous performance on different shipping routes has been ignored in past estimations of shipping emissions as well as in long-term shipping forecasts^{2,26}.

Global shipping trade-emissions matrix

The GTEMS achieves rationally interpreted trade-linked shipping emissions at the country level as it overcomes the uncertainty from the transshipment conundrum and non-loaded voyages in AIS-based models (Supplementary Discussion 2 and Supplementary Fig. 3). Figure 2a shows the global shipping CO₂ emissions driven by global trade flow aggregated at the bilateral level, where each entry in the matrix reveals the shipping emissions generated by maritime transportation of all traded commodities for each single-direction trade pair. Among thousands of emissions flows at the country level, the top 10 high-emissions flows collectively contribute to 17.2% of global shipping emissions, of which Brazil–China (5.4%), Australia–China (3.4%), United States–China (1.6%) and China–United States (1.3%) are notable high-value entries in the matrix. Meanwhile, the global emissions proportion of the top 10 trade flows at country level is approximately twice the contributions of their aggregated maritime trade value (9.4%), while each flow also shows divergent contributions in terms of maritime trade value, weight and associated

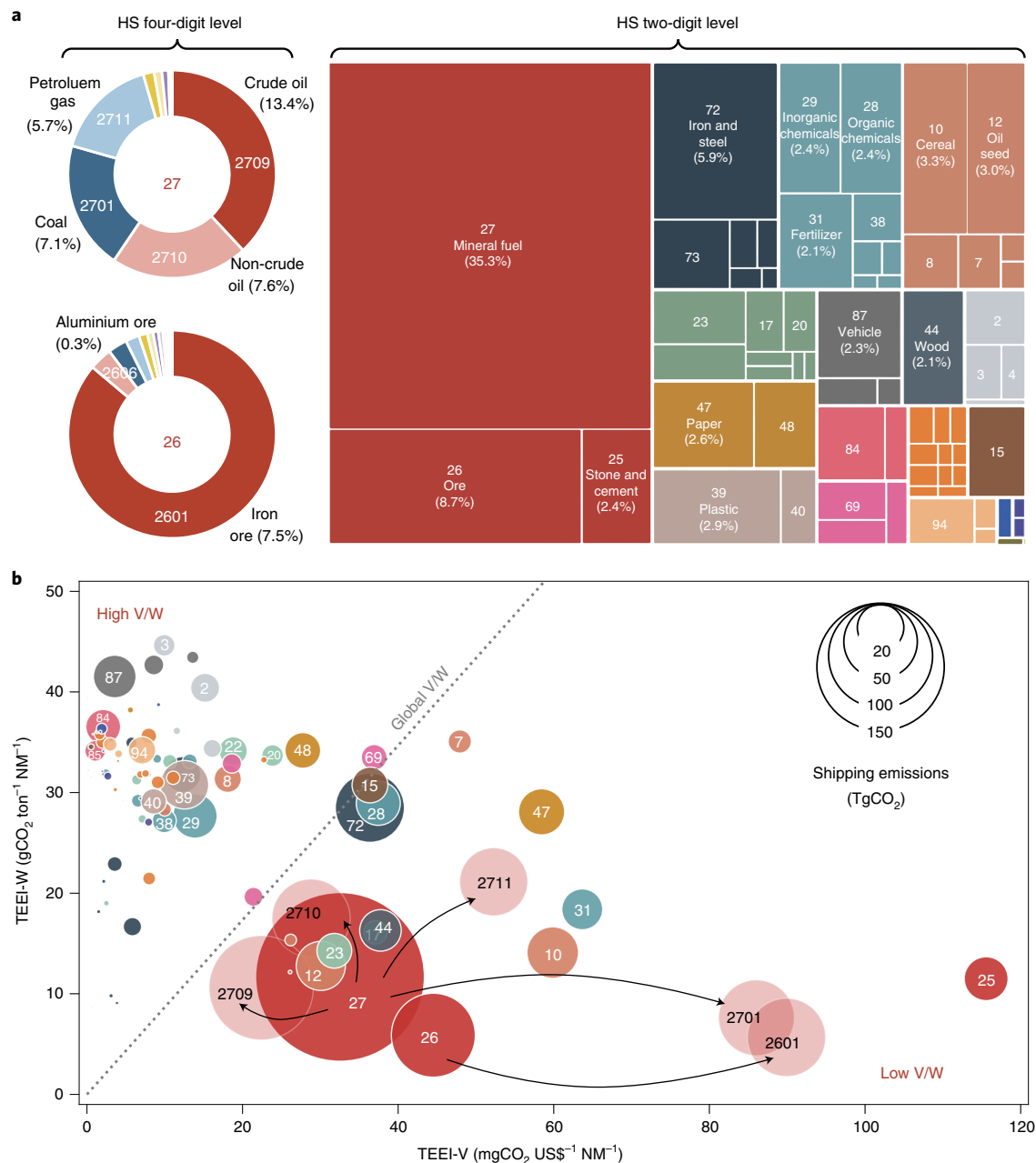


Fig. 3 | Characteristics of shipping CO₂ emissions of international trade commodities. a, Shipping emissions split by commodity chapters.

b, Trade-emissions efficiency indices of different commodities. The two-digit figures in both **a** and **b** refer to the HS two-digit level commodity chapters, and the colours indicate commodities belonging to different HS sections (roman numerals in Supplementary Table 3). The unmarked commodity chapters in **a** together contribute to <10% of total emissions. Commodities of HS 27 and HS 26 in **a** and **b** are further split into the HS 4-digit level.

shipping emissions (Supplementary Table 2). Such discrepancy demonstrates the inequality in contribution among traders in terms of the economic benefits brought by trade development and the negative impact on climate.

The quantitative decomposition of global shipping emissions into single-direction trade-pair flows consolidates the methodology and enhances transparency for international shipping emissions “allocation by trade”, option six proposed by the UNFCCC¹⁷. However, to yield a rational responsibility allocation, the factors that needed to be taken into consideration are far beyond the emissions interpreted in Fig. 2a. In terms of the accumulated shipping emissions by country, China is estimated to be the largest contributor from both the import and the export perspectives. However, as a

‘world factory’³⁹, the considerable proportion of shipping emissions attributed to China is induced by the import of mineral fuels and ores and the re-export of manufactured goods⁴⁰. From this point of view, shipping emissions driven by trade commodities may be attributed to far more countries than their directly related bilateral traders, since the beneficiaries also involve the upstream and downstream countries in the supply chain. It can be foreseen that shipping emissions allocation according to initial producers or final consumers may generate different responsibilities at the country level compared with those of the direct trade exporter and importer. Such discrepancy reveals the potential unfairness among countries in shipping emissions responsibility allocation by trade. However, for the moment, the GTEMS model marks an advance in

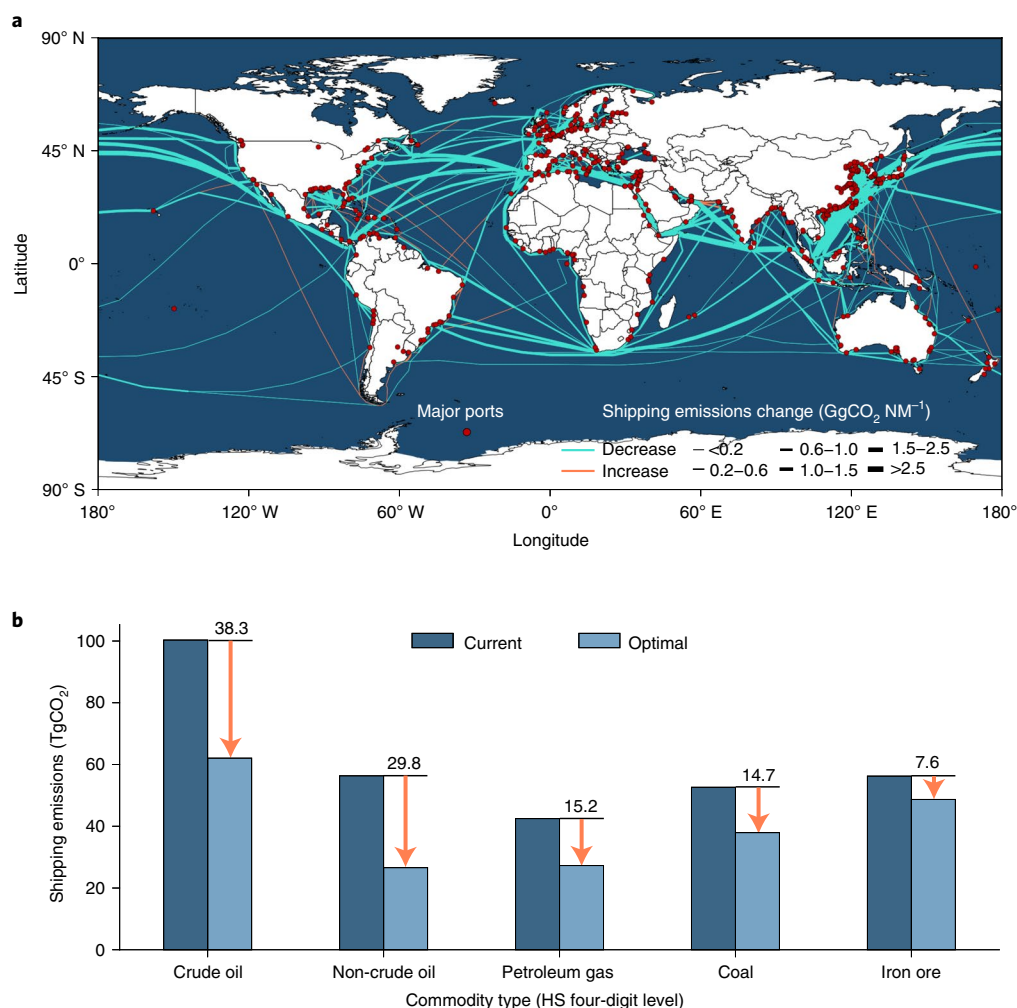


Fig. 4 | Shipping emissions changes in CO₂ by optimizing trade partners. a, b. Shipping emissions changes in CO₂ on shipping routes (**a**) and for major commodities (**b**) by optimizing trade partners. Numbers labelled in **b** show the absolute amounts of shipping CO₂ emissions reduction. Maps are made with Natural Earth.

decomposing global shipping emissions to trade pairs and exporters/importers, which could serve as an evaluation framework to support the cooperation of trade pairs on emissions reduction.

While the shipping emissions matrix in Fig. 2a reveals the aggregation of shipping needs, Fig. 2b,c, given by TEEI-W ($\text{gCO}_2 \text{ ton}^{-1} \text{ NM}^{-1}$) and trade-emissions efficiency index by value (TEEI-V; $\text{mgCO}_2 \text{ US\$}^{-1} \text{ NM}^{-1}$), enable understanding of the trade-related shipping emissions efficiency at the bilateral level. Due to the heterogeneities in international trade structures and vessel operating efficiency, the discrepancy in TEEI-W among different bilateral emissions flows reaches 38-fold ($4.7\text{--}175.7 \text{ gCO}_2 \text{ ton}^{-1} \text{ NM}^{-1}$). Countries with higher estimated TEEI-Ws are associated with more transportation by emissions-intensive vessels; this is especially the case for Germany, with its massive export of vehicles and large machineries carried out by Ro-Ro ships (Supplementary Fig. 1). This may somewhat explain the relatively high TEEI-W in European waters (Fig. 1b). Considering the economic value rather than weight, the variation in TEEI-V among different bilateral pairs is up to thousands of times ($0.1\text{--}865.6 \text{ mgCO}_2 \text{ US\$}^{-1} \text{ NM}^{-1}$), with a global average of 15.6 mg per US\$ in trade per nautical mile. Although Australia and Brazil have lower TEEI-Ws, their TEEI-Vs are notably high due to a large amount of low-cost and high-weight commodities exported. Considering the data accessibility issues involved in calculating TEEI-W and

TEEI-V, both the global-level and bilateral-level values of these indicators are provided here for potential application. With these multiscale indicators, the difficulty of building the nexus among economy, shipping and atmosphere is greatly reduced.

Shipping emissions of trade commodities

Figure 3a reveals the composition of international shipping CO₂ emissions by trade commodity chapter organized by the Harmonized System (HS). Among 98 commodity chapters at the HS 2-digit level, international freight transportation of mineral fuels (HS 27) contributes to 35.3% of shipping emissions. The major commodities at the HS 4-digit level are crude oils (HS 2709, 13.4%), non-crude oils (HS 2710, 7.6%), coals (HS 2701, 7.1%) and petroleum gases (HS 2711, 5.7%). Ores (HS 26) also account for another 8.7% of global shipping emissions, of which a majority are associated with iron ores (HS 2601, 7.5%). Other major contributors at the HS 2-digit level include irons and steels (HS 72, 5.9%), cereals (HS 10, 3.3%) and oil seeds (HS 12, 3.0%), and so on.

Figure 3b interprets the trade-emissions efficiencies for different commodities, each of which is a ratio of the total global shipping emissions involving all trade flows driven by this commodity to its total transport work. Bulk commodities dominated by mineral fuels (HS 27) and ores (HS 26), although contributing substantially to shipping emissions, have TEEI-Ws (mostly $<30 \text{ gCO}_2 \text{ ton}^{-1} \text{ NM}^{-1}$) that

are lower than those of most commodities, as these bulk products are generally carried by relatively energy-efficient bulk carriers and tankers (Supplementary Fig. 2). However, considering economic value, their lower unit prices would undoubtedly result in higher TEEI-Vs. In contrast, manufactured commodities, with relatively abundant categories by the HS system, are generally associated with higher TEEI-Ws due to transportation by energy-intensive containers and Ro-Ro ships (Supplementary Fig. 2) and lower TEEI-Vs (mostly $<20 \text{ mgCO}_2 \text{ US\$}^{-1} \text{ NM}^{-1}$) due to relatively higher economic values. In addition, the value/weight (V/W) difference of subchapters (HS 4-digit) compared with parent chapters (HS 2-digit) may lead to even larger deviations in TEEI-V, such as the cases of iron ore (HS 2601) and coal (HS 2701). It should be noted that the concept of the indices and the use of base data to calculate indices are of equal importance. Even for the same commodity, the discrepancy in fleet composition, ship operation efficiency and trade value among different trade pairs would lead to different TEEI estimation results on a global scale and for individual countries³⁴. Thus, the TEEI evaluated involving global trade flows is expected to provide more comprehensive quantitative parameters for shipping emissions evaluation on a global scale.

Trade-driven shipping emissions-reduction potential

Any changes to ship design and operation, trade partners, trade volume or trade structure could lead to changes in shipping emissions. The GTEMS model has the distinct advantage of tracking all the changes above and evaluating their effects on shipping emissions. A case is provided here to demonstrate one typical application of the GTEMS model. In this case, we evaluate the maximum emissions-reduction potential in an ideal scenario whereby all countries follow the principle of nearby trade (Methods). If the total import and export volume of each commodity is left unchanged but trading partners are optimized, the global shipping CO₂ emissions of international trade commodities can ideally be reduced by 38%, an amount equivalent to 284.0 Tg. The estimated emissions changes on shipping routes and the leading commodities are illustrated in Fig. 4. The shipping emissions intensity of most trade routes would be greatly relieved, and the peak shipping CO₂ emissions intensity could be minimized by 10.2 GgNM^{-1} . Major emissions-reduction efforts are driven by shipping optimization of crude oils, non-crude oils, iron ores, coals and petroleum gases, which contribute 38.3 Tg, 29.8 Tg, 15.2 Tg, 14.7 Tg and 7.6 Tg of CO₂, respectively. Among the major commodities, non-crude oil has the greatest emissions-reduction potential relative to itself, reaching a proportion of 52.8%, followed by crude oils (38.1%) and petroleum gases (35.8%).

Currently, more efforts are focused on improving the performance of ships. However, ships are at the end-of-pipe in global shipping, while trade demand is at the start. Achieving shipping emissions reduction through global trade optimization has never been dug up. This hypothetical scenario, as a tip of the iceberg, demonstrates the enormous shipping emissions-reduction potential that can be gained from changing the international trade pattern.

Discussion

Our study innovatively develops a compound technical framework, the VoySEIM–GTEMS model chain, by integrating data and methods from the fields of economy, transportation and atmospheric science, and finally decomposes global shipping emissions into disaggregated trade-linked emissions flows. This framework supplements recent insights from the fourth IMO GHG study with multiple key indicators and expands the understanding of international shipping emissions. The proposal of TEEI-V and TEEI-W for trade commodities and countries further improves the transparency in reflecting the trade-linked shipping emissions efficiency. This framework can be used to assess or predict the impact of trade events on shipping emissions, or assess the benefits brought by traders' contributions (country or company) and, finally, to

support integrated evaluations of emissions-reduction scenarios coupling economic and technological policies. It is hoped that the novel VoySEIM–GTEMS model chain developed in this study will serve as a benchmarking tool for supporting the construction of a systematic solution and joint efforts from the shipping industry and global trade network to address global climate change.

The heterogeneity in trade-linked shipping emissions efficiency among trade flows indicates the cumulative effect of the combination of ships, fleet routes and cargo. The most recent IMO GHG study suggests that the potential emissions reduction of the eight groups of profitable technical and operational measurements would be less than 10% until 2030 and 18% until 2050 (ref. ³). Under the current situation, where shipping decarbonization is mainly oriented by technical and operational measures on ships, our simulated trade scenario shows a huge potential for driving shipping emissions reduction (38%) by optimizing the international trade pattern. Results of this study can promisingly play an important role for scientists and policymakers in exploring multiple pathways for achieving the IMO's GHG emissions-reduction goal.

In addition, the VoySEIM–GTEMS model chain advances the research on emissions transfer embedded in the supply chain. On one hand, transport emissions are still treated as an external sector that has long been omitted in the supply chain. The VoySEIM–GTEMS model chain shows competency in evaluating transport-related emissions in the middle links of the supply chain, which overcomes the main shortcomings of the current accounting method that focuses mostly on production-related emissions^{41,42}. On the other hand, simply allocating emissions responsibility by bilateral trade is unfair to countries in the middle of the supply chain. Technical inputs are still needed to propose solutions to distinguish processing from terminal consumption.

Online content

Any methods, additional references, Nature Research reporting summaries, source data, extended data, supplementary information, acknowledgements, peer review information; details of author contributions and competing interests; and statements of data and code availability are available at <https://doi.org/10.1038/s41558-021-01176-6>.

Received: 18 December 2020; Accepted: 3 September 2021;

Published online: 7 October 2021

References

1. *Review of Maritime Transport 2019* (United Nations Conference on Trade and Development, 2019); https://unctad.org/en/PublicationsLibrary/rmt2019_en.pdf
2. *Fourth IMO Greenhouse Gas Study* (International Maritime Organization, 2020).
3. Bows-Larkin, A., Anderson, K., Mander, S., Traut, M. & Walsh, C. Shipping charts a high carbon course. *Nat. Clim. Change* **5**, 293–295 (2015).
4. Peters, G. P. et al. Carbon dioxide emissions continue to grow amidst slowly emerging climate policies. *Nat. Clim. Change* **10**, 3–6 (2020).
5. Crippa, M. et al. *Fossil CO₂ Emissions of All World Countries—2020 Report* (Publications Office of the European Union, 2020); https://edgar.jrc.ec.europa.eu/report_2020
6. Capaldo, K., Corbett, J. J., Kasibhatla, P., Fischbeck, P. & Pandis, S. N. Effects of ship emissions on sulphur cycling and radiative climate forcing over the ocean. *Nature* **400**, 743–746 (1999).
7. Doelle, M. The Paris Agreement: historic breakthrough or high stakes experiment? *Clim. Law* **6**, 1–20 (2016).
8. Traut, M. et al. CO₂ abatement goals for international shipping. *Clim. Policy* **18**, 1066–1075 (2018).
9. *Initial IMO Strategy on Reduction of GHG Emissions from Ships* MEPC.304(72) (Marine Environment Protection Committee, 2018); [https://wwwcdn.imo.org/localresources/en/KnowledgeCentre/IndexofIMOResolutions/MEPCDocuments/MEPC.304\(72\).pdf](https://wwwcdn.imo.org/localresources/en/KnowledgeCentre/IndexofIMOResolutions/MEPCDocuments/MEPC.304(72).pdf)
10. *2012 Guidelines of the Method of Calculation of the Attained Energy Efficiency Design Index (EEDI) for New Ships* MEPC.212(63); Annex 8 (Marine Environment Protection Committee, 2012); [https://wwwcdn.imo.org/localresources/en/KnowledgeCentre/IndexofIMOResolutions/MEPCDocuments/MEPC.212\(63\).pdf](https://wwwcdn.imo.org/localresources/en/KnowledgeCentre/IndexofIMOResolutions/MEPCDocuments/MEPC.212(63).pdf)

11. 2012 *Guidelines for the Development of a Ship Energy Efficiency Management Plan (SEEMP)* MEPC.212(63); Annex 9 (Marine Environment Protection Committee, 2012); [https://wwwcdn.imo.org/localresources/en/OurWork/Environment/Documents/213\(63\).pdf](https://wwwcdn.imo.org/localresources/en/OurWork/Environment/Documents/213(63).pdf)
12. *Guidelines for Voluntary Use of the Ship Energy Efficiency Operational Indicator* MEPC.213(65) (Marine Environment Protection Committee, 2009); <https://gm.imo.org/wp-content/uploads/2017/05/Circ-684-EEOI-Guidelines.pdf>
13. Shi, Y. Reducing greenhouse gas emissions from international shipping: is it time to consider market-based measures? *Mar. Policy* **64**, 123–134 (2016).
14. Bouman, E. A., Lindstad, E., Rialland, A. I. & Strømman, A. H. State-of-the-art technologies, measures, and potential for reducing GHG emissions from shipping—a review. *Transp. Res. D* **52**, 408–421 (2017).
15. Mallouppas, G. & Yfantis, E. A. Decarbonization in shipping industry: a review of research, technology development, and innovation proposals. *J. Mar. Sci. Eng.* <https://doi.org/10.3390/jmse9040415> (2021).
16. Balcombe, P. et al. How to decarbonise international shipping: options for fuels, technologies and policies. *Energy Convers. Manag.* **182**, 72–88 (2019).
17. *Report of its Subsidiary Body for Scientific and Technological Advice on the Fourth Session Held in Geneva from 16 to 18 December 1996* FCCC/SBSTA/1996/9/Add.1 (United Nations Framework Convention on Climate Change, 1996); <https://unfccc.int/documents/1439>
18. Corbett, J. J. & Fischbeck, P. Emissions from ships. *Science* **278**, 823–824 (1997).
19. Cadarso, M.-Á., López, L.-A., Gómez, N. & Tobarra, M.-Á. CO₂ emissions of international freight transport and offshoring: measurement and allocation. *Ecol. Econ.* **69**, 1682–1694 (2010).
20. Heitmann, N. & Khalilian, S. Accounting for carbon dioxide emissions from international shipping: burden sharing under different UNFCCC allocation options and regime scenarios. *Mar. Policy* **35**, 682–691 (2011).
21. Rahim, M. M., Islam, M. T. & Kuruppu, S. Regulating global shipping corporations' accountability for reducing greenhouse gas emissions in the seas. *Mar. Policy* **69**, 159–170 (2016).
22. den Elzen, M. G. J., Oilvier, J. G. J. & Berk, M. M. *An Analysis of Options for Including International Aviation and Marine Emissions in a Post-2012 Climate Mitigation Regime* (Netherlands Environmental Assessment Agency, 2007).
23. Selin, H., Zhang, Y., Dunn, R., Selin, N. E. & Lau, A. K. H. Mitigation of CO₂ emissions from international shipping through national allocation. *Environ. Res. Lett.* **16**, 045009 (2021).
24. Lee, T.-C., Lam, J. S. L. & Lee, P. T.-W. Asian economic integration and maritime CO₂ emissions. *Transp. Res. D* **43**, 226–237 (2016).
25. Cristea, A., Hummels, D., Puzzello, L. & Avetisyan, M. Trade and the greenhouse gas emissions from international freight transport. *J. Environ. Econ. Manag.* **65**, 153–173 (2013).
26. Martínez, L. M., Kaupilla, J. & Castaing, M. International freight and related carbon dioxide emissions by 2050. *Transp. Res. Rec.* **2477**, 58–67 (2015).
27. Yoon, Y., Yang, M. & Kim, J. An analysis of CO₂ emissions from international transport and the driving forces of emissions change. *Sustainability* <https://doi.org/10.3390/su10051677> (2018).
28. Stojanović, D., Ivetić, J. & Veličković, M. Assessment of international trade-related transport CO₂ emissions—a logistics responsibility perspective. *Sustainability* <https://doi.org/10.3390/su13031138> (2021).
29. Nunes, R. A. O., Alvim-Ferraz, M. C. M., Martins, F. G. & Sousa, S. I. V. The activity-based methodology to assess ship emissions—a review. *Environ. Pollut.* **231**, 87–103 (2017).
30. Johansson, L., Jalkanen, J.-P. & Kukkonen, J. Global assessment of shipping emissions in 2015 on a high spatial and temporal resolution. *Atmos. Environ.* **167**, 403–415 (2017).
31. Liu, H. et al. Health and climate impacts of ocean-going vessels in East Asia. *Nat. Clim. Change* **6**, 1037–1041 (2016).
32. Winther, M. et al. Emission inventories for ships in the Arctic based on satellite sampled AIS data. *Atmos. Environ.* **91**, 1–14 (2014).
33. Jalkanen, J. P., Johansson, L. & Kukkonen, J. A comprehensive inventory of ship traffic exhaust emissions in the European sea areas in 2011. *Atmos. Chem. Phys.* **16**, 71–84 (2016).
34. Schim van der Loeff, W., Godar, J. & Prakash, V. A spatially explicit data-driven approach to calculating commodity-specific shipping emissions per vessel. *J. Clean. Prod.* **205**, 895–908 (2018).
35. Liu, H. et al. Emissions and health impacts from global shipping embodied in US–China bilateral trade. *Nat. Sustain.* **2**, 1027–1033 (2019).
36. Adland, R., Jia, H. & Strandenes, S. P. The determinants of vessel capacity utilization: the case of Brazilian iron ore exports. *Transp. Res. A* **110**, 191–201 (2018).
37. Prill, K. & Igielski, K. Calculation of operational indicator EEOI for ships designed to other purpose than transport based on a research-training vessel. *New Trends Prod. Eng.* **1**, 335–340 (2018).
38. Streets, D. G., Guttikunda, S. K. & Carmichael, G. R. The growing contribution of sulfur emissions from ships in Asian waters, 1988–1995. *Atmos. Environ.* **34**, 4425–4439 (2000).
39. Liu, J. & Diamond, J. China's environment in a globalizing world. *Nature* **435**, 1179–1186 (2005).
40. Andersen, O. et al. CO₂ emissions from the transport of China's exported goods. *Energy Policy* **38**, 5790–5798 (2010).
41. Davis, S. J. & Caldeira, K. Consumption-based accounting of CO₂ emissions. *Proc. Natl Acad. Sci. USA* **107**, 5687–5692 (2010).
42. Peters, G. P. & Hertwich, E. G. CO₂ embodied in international trade with implications for global climate policy. *Environ. Sci. Technol.* **42**, 1401–1407 (2008).

Publisher's note Springer Nature remains neutral with regard to jurisdictional claims in published maps and institutional affiliations.

© The Author(s), under exclusive licence to Springer Nature Limited 2021

Methods

Technical framework and data sources. In this study, we construct a compound model chain (VoySEIM–GTEMS) to systematically investigate trade-linked shipping emissions and efficiencies for different bilateral pairs and commodities in global maritime trade with a target year of 2018. The structure and the integration methods of the two models are shown in Supplementary Fig. 4. The VoySEIM is an extended model based on our previous bottom-up Ship Emission Inventory Model (SEIM)³¹, in which a voyage identification method is added to estimate voyage-based shipping emissions and EEOIs occurring between the departure and arrival countries. It should be noted that an observed voyage is not exactly associated with the trade export between the departure and the arrival countries. Therefore, instead of directly adopting voyage-based emissions, we develop a GTEMS model to estimate trade-linked shipping emissions by taking the multitudinous trade flows as driving data and combining with the voyage-based EEOI obtained from the VoySEIM.

The construction of the VoySEIM–GTEMS model requires commercial ship data and freely available trade datasets. The commercial ship data include: (1) the AIS data for the whole year of 2018 (from 1 January to 31 December), which provide high-frequency vessel activity information (31 billion signals) including signal time, coordinate location, navigational speed, operating status and so on, and (2) the integrated Ship Technical Specifications Database (STSD, also updated to 2018), which describes ship static properties including vessel type, DWT, engine power and so on. Our previous work has discussed the detailed processing method of the AIS data collection, cleaning, matching and verification³¹. Non-cargo ships not related to international trade, for example, cruise ships and fishing ships, are excluded.

The trade data from 2018 were mainly collected from the Base pour l'Analyse du Commerce International (BACI) database developed by Le Centre d'études prospectives et d'informations internationales (CEPII; <http://www.cepii.fr>), which provides yearly bilateral trade value and quantity for more than 5,000 commodities from over 200 countries. Commodities are organized according to the HS code, which is arranged in 98 chapters (HS first 2 digits) and grouped in 22 sections (Supplementary Table 3). Due to the similarity of over-classified commodities in terms of transport vessels and emissions characteristics, the original commodities were merged at the HS four-digit level. At the same time, countries with unremarkable maritime trade and gross domestic products were incorporated into "others". The detailed preprocessing steps for the BACI trade data, including national filtering principles, are described in Supplementary Methods 1. After the preprocessing, a total of 1.2 million trade flows (a certain category of commodity exported from one country to another) were obtained, which is composed of 2,451 bilateral exporter–importer flows at the country level (49 major maritime countries and one "others") and over 1,200 commodities. Supplementary Table 4 lists the statistics of merged trade import and export by country in 2018. To estimate the proportion of seaborne trade from the BACI data, we further collected the modal-split trade data from the United Nations (UN) Comtrade database (<https://comtrade.un.org/data>), the Eurostat database (<https://ec.europa.eu/eurostat/data/database>) and the US census (<https://usatrade.census.gov>). These data record trade items by mode of transport.

Global voyage-based EEOI calculation. The international voyage is defined here as observed shipping routes between different departure and the arrival countries, which can be identified by the dynamic changes of vessel speed and location from AIS data. The technical details for identifying the shipping voyage are described in Supplementary Methods 2. Shipping emissions can be estimated for each time interval of two consecutive AIS signals based on the ship's instantaneous engine power and the power-based emissions factors and then aggregated for each voyage. The cargo mass transported for a particular voyage is calculated with the DWT provided by STSD and the loading efficiencies⁴³. Since the AIS signal continuously reports the vessel's position (longitude and latitude), the voyage distance can be calculated by applying the great-circle distance algorithm to the position sequence and accumulating the results from all segments. Therefore, the voyage-specific EEOI is calculated by equation (1).

$$\text{EEOI}_{v,s,i} = \frac{E_{v,s,i} \times (1 + \text{BAF}_{v,s})}{\text{DWT}_i \times \text{TCU}_{v,s} \times D_{v,s,i}} \times 10^6 \quad (o \neq d) \quad (1)$$

where $\text{EEOI}_{v,s,i}$ is the energy efficiency operational indicator for each voyage i , classified by vessel type v and size bin s , in $\text{gCO}_2 \text{ ton}^{-1} \text{ NM}^{-1}$; $E_{v,s,i}$ is the estimated shipping CO_2 emissions by voyage i , classified by vessel type v and size bin s , in tonnes; $\text{BAF}_{v,s}$ is the berthing adjust factor for vessel type v and size bin s (refer to DWT range), and is unitless; DWT_i is the vessel's dead weight tonnage of voyage i , independent of the dynamic activities, in tonnes; $\text{TCU}_{v,s}$ is the total capacity utilization for vessel type v and size bin s , and is unitless, and $D_{v,s,i}$ is the shipping distance of voyage i , classified by vessel type v and size bin s , in NM. The shipping emissions incorporate those from the main engines, auxiliary engines and boilers.

To provide input parameters for the GTEMS model, the voyage-based EEOIs were averaged by vessel type and the o – d country pair, as shown by equation (2).

$$\text{EEOI}_{v,o,d} = \frac{\sum_s \sum_i [E_{v,s,o,d,i} \times (1 + \text{BAF}_{v,s})]}{\sum_s (\text{DWT}_i \times \text{TCU}_{v,s} \times D_{v,s,o,d,i})} \times 10^6 \quad (o \neq d) \quad (2)$$

where $\text{EEOI}_{v,o,d}$ is the total weighted energy efficiency operational indicator of vessel type v navigating between country o and country d ($o \neq d$, the same as below), in $\text{gCO}_2 \text{ ton}^{-1} \text{ NM}^{-1}$; $E_{v,s,o,d,i}$ is the estimated shipping CO_2 emissions by voyage i between country o and country d , classified by vessel type v and size bin s , in tonnes, and $D_{v,s,o,d,i}$ is the shipping distance of voyage i between country o and country d , classified by vessel type v and size bin s , in NM.

TCU. In this study, a parameter of TCU is introduced to describe a vessel's actual transport work versus its maximum transport capacity. For each vessel type and size bin, the TCU is estimated as the product of the allocative utilization (ratio of total loaded distance to total distance) and payload utilization (ratio of the average payload mass to the DWT of the ship), which were collected from the University College London (UCL)'s (2015) study⁴³. In this way, the TCU considers the vessel ballast conditions, multiple port deliveries as well as typical capacity utilizations when loaded. For vessel types currently not available for TCU, a default value of 70% would be applied. As for container vessels, the TCU was further adjusted by a factor of 85%, considering the net weight of the empty container¹². Supplementary Table 5 shows the final TCUs applied in this study. By applying the TCU, the total cargo transported for each vessel type can also be aggregated for verification (the 'Quality assurance/quality control and validations' section).

BAF. In the VoySEIM, the voyage directly identified only includes the cruising and manoeuvring modes of ships in international transportation, while ignoring their berthing and anchorage modes. Therefore, a BAF is introduced to adjust the result of voyage-based emissions, which is defined as the ratio of emissions generated during ships' berthing and anchorage modes to those during cruising and manoeuvring modes. The BAF can be calculated from the aggregate results from the SEIM model¹³ (Supplementary Table 6), assuming it varies with vessel type and size due to different cargo handling time.

International trade-driven shipping emissions estimation. Based on the bilateral trade flow and the fleet energy efficiency resulting from the VoySEIM, the GTEMS model was established to estimate international trade-linked shipping emissions. In this model, the maritime commodities are assumed to be transported on simulated bilateral trading routes. Beginning with the pre-processed bilateral trade data obtained from the BACI database, the volume of seaborne trade was first separated from that of all modes of transportation. Then, each seaborne trade flow was matched to the appropriate type of transport vessel. Combined with the EEOI and the bilateral route distance, shipping emissions driven by each trade flow can be finally achieved. The general formula in the GTEMS model is shown in equation (3):

$$E_{o,d,c,v} = W_{o,d,c} \times \text{SP}_{o,d,c} \times \text{VD}_{c,v} \times \text{EEOI}_{v,o,d} \times D_{o,d} \times 10^{-6} \quad (o \neq d) \quad (3)$$

where $E_{o,d,c,v}$ is the shipping CO_2 emissions driven by trade commodity c from country o to country d and transported by vessel type v , in tonnes; $W_{o,d,c}$ is the total weight of trade commodity c exported from country o to country d , in tonnes; $\text{SP}_{o,d,c}$ is the seaborne proportion of trade commodity c exported from country o to country d , and is unitless; $\text{VD}_{c,v}$ is the vessel distribution coefficient of trade commodity c carried by vessel type v , and is unitless; $\text{EEOI}_{v,o,d}$ is the energy efficiency operational indicator for vessel type v voyaging from country o to country d , in $\text{gCO}_2 \text{ ton}^{-1} \text{ NM}^{-1}$, and $D_{o,d}$ is the shipping distance from country o to country d on a standardized route network, in NM.

Seaborne trade proportion. The SP for each trade commodity of each country pair is determined by either direct calculation or indirect estimation. According to other modal-split trade data collected from the UN Comtrade, Eurostat and the US census, the direct calculation method could be applied to approximately 68% of the global trade volume. For the remaining part, we assume that the selection of transportation mode depends on land transportation availability and the commodity characteristics. A land transport infeasibility index (LTII) is first introduced to describe the possibility of land transportation of goods between trading partners. When this value is set to 1, it means that the country pair is basically transoceanic. In this case, we assume the possibility of choosing sea or air transportation for trade goods would depend on its own feature. This could be demonstrated by the estimated seaborne proportion (SP') of transoceanic country pairs based on the available modal-split data (Supplementary Fig. 5). Finally, the product of these two ratios is used to estimate the indirect SP, as illustrated in equation (4).

$$\text{SP}_{o,d,c} = \text{SP}'_c \times \text{LTII}_{o,d} \quad (o \neq d) \quad (4)$$

where $\text{SP}_{o,d,c}$ is the seaborne proportion of commodity c exported from country o to country d ; SP'_c is the seaborne proportion of commodity c , pre-estimated based on transoceanic countries in modal-split trade data, and $\text{LTII}_{o,d}$ is the land transport infeasibility index from country o to country d .

Technical details about the SP investigation, estimation and verification are described in Supplementary Methods 3 and Supplementary Figs. 5 and 6. The estimated seaborne proportion of global international trade volume for different commodity chapters as well as the OD matrices of maritime trade values and quantities are summarized in Supplementary Fig. 7.

Commodity–vessel linkage. The linking approach of commodities to vessel types has been preliminarily established in our previous study for the US–China bilateral trade²⁴. In this study, we expanded the linking approach to the global scale. By summarizing the logistics information collected from the marine logistics information platform website (<http://company.shipping.jctrans.com>), we developed a set of distribution coefficients for each commodity (at the HS four-digit level) to be allocated to different transport vessels. Supplementary Fig. 8 shows the leading transport vessel type for each commodity chapter and the estimated commodity–vessel transportation flows. Containers are the leading transport vessels for most manufactured commodities. Coals, ores and other raw materials in section V, accounting for the largest proportions of seaborne trade volume, are typically transported by bulk carriers. Oil tankers are responsible for the transportation of crude oils and oil products (for example, HS 2709 and HS 2710), while liquid gas tankers are responsible for that of petroleum gases and natural gases (for example, HS 2711). Chemical tankers are widely used to carry toxic, flammable or corrosive chemical products, for example, some of the chapters in section VI. Reefers (refrigerated ships) are mainly used to carry perishable commodities, for example, some of the chapters in section I. Vehicles in section XVII and large mechanical equipment in section XVI are generally matched to Ro-Ro ships.

Shipping route distance. Although some previous studies have incorporated the bilateral trade distance for trade-related simulations of shipping emissions^{24,25}, most of them used the ground distance between the capitals or mega-cities rather than the actual shipping distance. To accurately estimate shipping emissions in the GTEMS model, we extracted the spatial information from the AIS data to develop a global shipping route network and simulate the most representative bilateral route distance. Based on the aggregated spatial pattern of all AIS signals, the shipping routes were drawn arc by arc, with a total of 3,570 arcs connected by 2,470 nodes. Regarding the global shipping route network as an undirected graph, the shortest path between each set of two nodes and the geodesic distance could be calculated using the Dijkstra shortest-path algorithm⁴⁴. In this way, a total of 246,017 port-to-port shortest routes were obtained for the world's top 500 coastal ports (Supplementary Fig. 9). Since trading countries generally have multiple ports, the shipping route between each country pair may have various options. A simple average of all route distances may bring large deviations to countries with long coastlines or widely distributed ports, such as the United States, Canada and Russia. To address this, several tests were carried out by comparing the estimated bilateral route distances based on Dijkstra algorithm with the abundant observed shipping distances calculated by the VoySEIM. The results demonstrated that the tests obtained the best coefficient of determination ($R^2=0.83$) and the mean square error ($MSE=0.60$) at the 10% quantile (Supplementary Fig. 9). In addition, shipping distances of the simulated routes were generally lower than the observed voyages, as they ignored the interference of wind and waves occurring with actual conditions. Thus, we eventually rectified these downward deviations, assuming they were balanced between different trading pairs.

Decarbonization potential by optimizing trading partners. As a typical application of the GTEMS model, we simulated the shipping emissions-reduction potential of redistributing trading partners while ensuring the current international trade volume. When each country imports/exports similar commodities to partners with closer route distance and/or chooses routes with better energy efficiency, it is possible to achieve shipping emissions reduction. This case can be regarded as a linear programming model. In this model, the objective function is to minimize the total emissions of international shipping, and the constraint conditions are that the total import volume (weight) and the total export volume (weight) of each country's maritime trade remain unchanged. These constraints are to ensure that the flow of trade goods will not exceed the production capacity and demand of any country. In this simulation scenario, other factors such as costs, international relations, trade policies and so on are not considered. Given each commodity c and its current seaborne trade weight matrix, the decision variables are considered as a new seaborne trade weight matrix and the objective function can be expressed as equation (5), which is subject to equation (6).

$$E_{\min} = \sum_c \sum_{o,d} \sum_v SW'_{o,d,c} \times VD_{c,v} \times EEOI_{v,o,d} \times D_{o,d} \times 10^{-6} \quad (o \neq d) \quad (5)$$

$$s.t. \begin{cases} \sum_d SW'_{o,d,c} \leq \sum_d SW_{o,d,c} \quad (o = 1, 2, \dots, 50) \\ \sum_o SW'_{o,d,c} \leq \sum_o SW_{o,d,c} \quad (d = 1, 2, \dots, 50) \\ \sum_{o,d} SW'_{o,d,c} = \sum_{o,d} SW_{o,d,c} \\ SW'_{o,d,c} = 0 \quad (o = d) \\ SW'_{o,d,c} \geq 0 \quad (o \neq d) \end{cases} \quad (6)$$

where E_{\min} is the minimum total international shipping CO₂ emissions, in tonnes; $SW_{o,d,c}$ is the current weight of seaborne trade commodity c exported from country o to country d , in tonnes; $SW'_{o,d,c}$ is the optimal weight of seaborne trade

commodity c exported from country o to country d , unit in ton; $VD_{c,v}$ is vessel distribution coefficient of commodity c carried by vessel type v , and is unitless; $EEOI_{v,o,d}$ is the shipping energy efficiency operational indicator for vessel type v voyaging from country o to country d , in gCO₂/ton¹NM⁻¹, and $D_{o,d}$ is the shipping distance from country o to country d , in NM.

Uncertainties. Uncertainties in the voyage-based EEOI calculation using the VoySEIM mainly come from the principle of voyage identification. First, since the voyage identification method is based on the dynamic change in vessel speed, the accuracy of this method largely relies on the quality of AIS data. Signal loss occasionally occurs in some regions with rare AIS base stations, such as the Middle East, resulting in the voyage being misidentified to other countries or dropped. Second, the delimitation of coastal boundaries directly affects the results of identified voyages. For neighbouring countries with narrow waters, especially European countries, voyages between countries are difficult to distinguish. Third, the domestic legs of international voyages related to the cargo transshipment are not taken into account in this identification method. Besides, countries with less trade volume are merged by continent, causing a small number of voyages between these countries to be ignored. In addition, it is obvious that more ship voyages than domestic trade demand are identified for cargo transit countries, such as Singapore, resulting more voyage-based shipping emissions (Supplementary Fig. 3). However, despite more samples for estimating voyage-based EEOI, the final trade-linked emissions in GTEMS would not be biased, because they are estimated based on bilateral trade data.

The construction of the GTEMS model is also subject to a few limitations. First, since the detailed commodity information is not available from the ship AIS data, there is a certain degree of inaccurate matching between the assumed vessels and the actual transport vessels. Second, the trade distance is considered to be independent of vessel type and commodity category, which may lead to the underestimation of the shipping distance for goods requiring multiple transshipments. At the same time, the unified rectification of the simulated route distance may result in different degrees of deviations for different trade pairs. Third, for trade pairs without identified voyages from the VoySEIM, the EEOI is assumed to be the global average. However, this potential deviation occurs only in a few country pairs that contribute little to total shipping emissions.

Quality assurance/quality control and validations. Throughout model development, the intermediate parameters and final results have been validated by quality assurance and control and compared with external sources to minimize uncertainties. Some intermediate parameters of the GTEMS have been validated step-by-step in Methods, including the seaborne trade proportion, commodity–vessel linkage and bilateral trade route distance. Other considerations are listed as follows.

First, a series of filters were applied to reduce the deviation of international voyage identification and EEOI estimation caused by unreliable ship data. (1) Vessels with incomplete technical information were excluded. (2) Voyages with the departure point or arrival point not within the coastal boundaries were filtered out to avoid being interrupted due to abnormal speed in AIS signals. (3) In the distribution of the estimated EEOI of all voyages, values less than the 0.5% quantile and values greater than the 0.95% quantile were filtered out to eliminate the interference of abnormal values. Results of the estimated EEOI were compared with the fourth IMO GHG study⁴, where the median and overall variation trend for each vessel type and size bin were generally similar (Supplementary Table 7).

Second, the estimated results of seaborne trade volume allocated to transport vessels in GTEMS were consistent with the vessel transport volume observed in the VoySEIM as well as the macro statistics (Supplementary Fig. 10). It was estimated that a total of 10.6 billion tonnes of commodities were transported by sea, which was highly consistent with the UN's maritime transport statistics, in which 11.0 billion tons of cargoes were loaded in the same year¹. In terms of commodity weight, 45.2% of maritime trade was transported by bulk carriers, followed by oil tankers (22.1%) and containers (15.8%), both of which were comparable with the statistics in maritime reports^{1,45}. As for the trade value, containers carried a majority of commodities (51.4%), which was also consistent with Clarkson's statistics (<https://www.clarksons.com/services/broking/containers/>).

Third, the shipping emissions results from GTEMS and the VoySEIM were compared with external work for verification. At the global scale, the total international shipping emissions resulting from GTEMS and the VoySEIM classified by ship type were similar to the latest assessment conducted by IMO using an analogous voyage-based method² (Supplementary Table 1 and Supplementary Fig. 10). At the finer scale, the results of shipping emissions at the bilateral and commodity levels could also be well verified by comparing with a case study for Brazilian exports (Supplementary Methods 4 and Supplementary Fig. 11).

Data availability

The AIS data and STSD are restricted to the third party and used under licence for the current study. Trade data including the BACI database (http://www.cepii.fr/CEPII/en/bdd_modelle/presentation.asp?id=37), UN Comtrade database (<https://comtrade.un.org/data/>), the US census (<https://usatrade.census.gov/>) and the Eurostat database (<https://ec.europa.eu/eurostat/data/database>) are all publicly available, with details described in the Methods. Emissions data are available from the corresponding author upon request. Source data are provided with this paper.

Code availability

Python codes used during the current study are available from the corresponding author on reasonable request.

References

43. *The Existing Shipping Fleet's CO₂ Efficiency* (UCL Energy Institute, 2015); <https://wwwcdn.imo.org/localresources/en/MediaCentre/HotTopics/Documents/MEPC%2068%20INF%2024%20REV1%20The%20existing%20shipping%20fleet%20CO2%20efficiency.pdf>
44. Cherkassky, B. V., Goldberg, A. V. & Radzik, T. Shortest paths algorithms: theory and experimental evaluation. *Math. Program.* **73**, 129–174 (1996).
45. *Shipping Statistics Yearbook* (Institute of Shipping Economics and Logistics, 2017).

Acknowledgements

This work is supported by the National Natural Science Foundation of China (grant nos. 41822505 and 42061130213 to H.L.). H.L. is supported by the Royal Society of the United Kingdom through a Newton Advanced Fellowship (NAF\R1\201166).

Author contributions

X-T.W. and H.L. designed the research and wrote the manuscript. X-T.W., Z-F.L. and F-Y.D. developed the VoySEIM model and conducted the shipping efficiency estimation. X-T.W. and H-L.X. developed the GTEMS model. Z-F.L., F-Y.D., L-J.Q., M-S.S. and S-X.Z. performed the analyses. H-Y.M. and K-B.H. provided insights into the scenario design. All authors contributed to the writing.

Competing interests

The authors declare no competing interests.

Additional information

Supplementary information The online version contains supplementary material available at <https://doi.org/10.1038/s41558-021-01176-6>.

Correspondence and requests for materials should be addressed to Huan Liu.

Peer review information *Nature Climate Change* thanks James Corbett and the other, anonymous, reviewer(s) for their contribution to the peer review of this work.

Reprints and permissions information is available at www.nature.com/reprints.